

Contrast-enhanced computed tomography features of oblique and straight distal sesamoidean ligament injury in thirty-one horses

Contrast-computertomografische bevindingen bij letsels van de schuine en rechte distale sesamsligamenten bij eenendertig paarden

¹L. Rasmussen, ¹J. H. Saunders, ³H. Van der veen, ¹E. Raes, ²E. Van veggel, ¹K. Vanderperren

¹ Department of Medical Imaging and Small Animal Orthopedics, Faculty of Veterinary Medicine, Ghent University, Belgium

² Sporthorse Medical Diagnostic Centre, Hooge Wijststraat 7, 5384 RC, Heesch, the Netherlands

³ Lingevoeve Diergeneeskunde, Veldstraat 3a, 4033 Lienden, the Netherlands

lisenr@gmail.com

ABSTRACT

Distal sesamoidean ligament (DSL) injury is a recognized cause of lameness in horses. The purpose of this study was to describe the contrast-enhanced computer tomography (CE-CT) findings in horses with injury to the DSL compared to a control group without injury to the DSL. Medical records of horses referred for CE-CT between 2008 and 2015 were reviewed. Cases were selected retrospectively based on a CE-CT imaging finding of injury to the DSL. Three horses had DSL injury as the only finding, while the remaining horses had one or more concomitant injuries. DSL injury and fetlock trauma and/or suspensory branch desmitis were the most frequent injury combinations. CE-CT can be of value in diagnosing DSL injury. The high number of concurrent DSL and fetlock and/or suspensory lesions suggests that further investigation should be considered when evaluating horses with injuries related to either of these structures.

SAMENVATTING

Letsels van de distale sesamligamenten (DSL) zijn een mogelijke oorzaak van claudicatie bij het paard. Het doel van deze studie was het beschrijven van de bevindingen tijdens contrast-computertomografisch onderzoek (CE-CT) bij paarden met letsels van de DSL in vergelijking met een controlegroep. De medische gegevens van paarden doorgestuurd voor een CE-CT-onderzoek tussen 2008 en 2015 werden verzameld. De gevallen werden retrospectief geselecteerd op basis van een letsel ter hoogte van de DSL vastgesteld met CE-CT. Drie paarden hadden enkel een letsel ter hoogte van de DSL, de overige paarden hadden één of meerdere bijkomende letsels. Letsels van de DSL met een trauma van de kogel en/of desmitis van de interosseustak waren de meest voorkomende combinaties van letsels. CE-CT is een waardevolle techniek om letsels van de DSL te diagnosticeren. Het hoge aantal gecombineerde letsels van de DSL en kogel en/of interosseous suggereert dat verder onderzoek raadzaam is wanneer paarden geëvalueerd worden met letsels in deze structuren.

INTRODUCTION

The distal sesamoidean ligaments (DSL) are part of the suspensory apparatus, stabilizing the metacarpo-/metatarsophalangeal (MCP/MTP) joint and preventing hyperextension of the MCP/MTP and proximal interphalangeal joint during loading of the limb. The DSL comprise the straight (SSL), the paired oblique (OSL), paired short and paired cruciate sesamoidean

ligaments. The SSL originates at the distal aspect of the proximal sesamoid bones and the intersesamoidean ligament, and inserts via the scutum medium on the palmaroproximal aspect of the middle phalanx together with the branches of the superficial digital flexor tendon. The lateral and medial OSL originate from the distal aspect of the lateral and medial proximal sesamoid bone respectively, and extend distally in an oblique manner to insert on the palmar/plantar

aspect of the proximal phalanx. The normal anatomic appearance of the DSL has been described using ultrasound, computed tomography (CT) and magnetic resonance imaging (MRI) (Denoix et al., 1991; Dyson et al., 1995; Smith et al. 2008a; Vanderperren et al., 2008). The challenging anatomical features of the pastern region complicates a thorough ultrasonographic evaluation and accurate lesion detection of the DSL. Injuries to the DSL has been described as a cause of lameness in the athletic horse; however, the publications are few (Dyson et al., 1995, Schneider et al., 2003; Marnieris et al., 2014).

The detection of injuries to the OSL and SSL using MRI has been described (Sampson et al., 2007; Smith et al., 2008a) showing promising results. Contrast media improve the clinical utility of CT by increasing the conspicuity of soft tissue lesions (Pollard et al., 2011). Contrast-enhanced computed tomography (CECT) has been demonstrated to accurately detect deep digital flexor tendon lesions when compared to histopathology and MRI, and allows additional characterization of the tendon lesion in regard to changes in vessel permeability and/or evidence of vascularization compared to MRI (Puchalski et al., 2009). To the authors knowledge, there is currently no research published describing CECT of DSL injury.

The objectives of this study were to describe the CECT features of the injured SSL and OSL in the horse.

MATERIAL AND METHODS

Medical records of all horses referred for CECT imaging of the distal limb, at the Lingehoeve Diergeneeskunde, the Netherlands, between 2008 and 2015 were used in this retrospective study. Cases were selected based on a CT imaging finding of injury to the DSL alone or in association with other injuries.

Horses presented with lameness localized to the distal limb by clinical examination (palpation; walk and trot on a circle on hard and soft ground, straight line on hard ground; flexion test of the distal limb evaluated on a straight line on hard ground) with/without diagnostic anesthesia of the distal limb. Diagnostic analgesia was not performed in cases with suspicion of incomplete fracture of the proximal phalanx.

Ten horses were selected as a control group. The control horses were selected based on clinical examination, response to local anesthesia and CT imaging findings that were unassociated with the DSL.

All control horses had lameness related to significant injury in the foot unassociated to the DSL, such as a fracture of the distal phalanx, or lameness that responded to either intraarticular anesthesia of the distal interphalangeal joint or anesthesia of the navicular bursa. The normal DSL were used as reference for comparison, as only CT examination of the lame limb of included horses was performed.

CT examination was performed with a 4-detector row helical CT scanner (MX 8000)a. Each horse was induced and maintained under general anesthesia using routine techniques (Bergman et al., 2007). The horses were positioned in lateral recumbency with the affected limb on the dependent side. The limb was positioned with the long axis of the limb perpendicular to the gantry of the CT scanner. Ultrasound guided catheterization of the median or cranial tibial artery, after aseptic preparation, was performed to enable intraarterial contrast delivery. Intraarterial contrast delivery was performed using 120 mL iodinated contrast medium (Ioversol, Optiray™ 350) diluted 1:1 with sterile saline (Puchalski et al., 2007). CT image acquisition parameters were 120 kV, 352 mAs, 2 mm slice thickness, 0.6 mm increment, 1-second rotation time, pitch of 0.88, SFOV of 10 cm, and matrix size of 512 X 512. The same parameters were used for the CECT. Transverse, reformatted sagittal and dorsal images were reviewed using bone and soft tissue settings.

The imaging studies were reviewed prospectively by the attending clinician and retrospectively by an ECVDI resident in training. Image interpretation was performed on a dedicated workstation using DICOM viewing (Osirix).

The following criteria were assessed and recorded for the CT studies using the control group as a reference: soft tissue swelling (presence or absence), osseous abnormalities on the proximal sesamoid bones, the proximal and the middle phalanx related to the attachment sites of the SSL and OSL (normal smooth outline or new bone formation), size (subjectively decreased, normal, increased), shape (normal, abnormal), margins (ill-defined or well-defined), pre-contrast CT density (subjectively decreased, normal, increased) and contrast enhancement. Contrast enhancement was defined as the mean attenuation (Hounsfield units (HU)) of the affected part of the ligaments using the region of interest (ROI) tool. The criteria for contrast enhancement was defined as no enhancement (less than 125 (OSL) or 118 (SSL) HU), mild enhancement (<20% affected and/or <200 HU), moderate enhancement (20-50% affected and/or 200-400 HU) or marked enhancement (>50% affected and/or >400 HU). The mean postcontrast attenuation (HU) of the control horses was calculated as a reference. Other osseous and ligamentous abnormalities were recorded both on CT and CECT, as well as abnormalities detected within additional structures.

Image evaluation was performed in transverse, sagittal and dorsal reconstructions, aligned with the orientation of the specific structure of interest (OSL or SSL).

The images were evaluated using both a soft tissue and bone window and level settings, but allowed to be altered by the reviewer as needed to best evaluate the structures of interest.

The lateral oblique sesamoidean ligament (LOSL),

medial oblique sesamoidean ligament (MOSL) and SSL were evaluated at the following locations:

Proximal region: immediately distal to the proximal sesamoid bones, at the point where the ligaments could first be clearly visualized.

Distal region: for the OSLs, the distal location was determined as the most distal point where the ligaments could be accurately separated as two individual structures. The distal location for the SSL was determined as the most distal point where the ligament could be visualized before forming the middle scutum.

Mid region: determined as the calculated intermediate point between the distal measurement and the base of the proximal sesamoid bones.

RESULTS

From all horses that underwent a CECT examination during 2008 and 2015, 31 had injury to the SSL or OSL and met the criteria for inclusion in this study. Age ranged from 2 to 16 years (mean 10.5 years, standard deviation 3.3 years; median 10.5 years). The age was unknown in one case.

The gender distribution was sixteen geldings, eleven mares and four stallions. There were twenty warmbloods, five ponies, two Icelandic, one Arabian, one Tinker, one quarter horse and one Haflinger.

All horses were examined because of lameness. The duration of clinical signs was variable (three to 16 weeks; mean 6.4 weeks, standard deviation 3.2 weeks), and in 17 horses the duration of lameness was not known. A positive response to a palmar digital nerve block was seen in five horses, to an abaxial sesamoid nerve block in two horses, a low palmar (low 4-point) in four horses, intraarticular anesthesia of the fetlock joint in four horses, anesthesia of the DFTS in one horse, and in fifteen horses, was either not performed (horses with suspicion of incomplete fracture of the proximal phalanx) or performed by the referring veterinarian (unspecified positive distal limb anesthesia).

Twenty-six horses had forelimb lameness (thirteen left front and thirteen right front) and five horses had hindlimb lameness (one left hind and four right hind).

The control group consisted of seven warmbloods, two ponies and one quarter horse.

Age of the control horses ranged from 1 to 16 years (mean 8.1 years; standard deviation 4.4 years, median 7.5 years). All control horses had front limb examinations (six right front and four left front).

CE-CT lesions were detected in the OSL in 28 horses and in the SSL in 13 horses. Abnormalities of only the OSL were seen in 18 horses and of only the SSL in three horses. A combination of abnormalities of the OSL and SSL were seen in ten horses.

Twenty-four horses had injury to the LOSL and

twenty horses to the MOSL. Eight horses had only LOSL injury, four only MOSL and sixteen were both LOSL and MOSL, resulting in a total of 44 injured OSLs.

Twenty-four horses had abnormalities involving the proximal part, 25 the middle part and 5 the distal part of the OSLs. Injury to the proximal part alone was seen in three cases and the middle alone in 4 cases. No injury was seen within the distal region alone. Combinations of the three regions were seen in 21 cases.

Only three horses had injury to the DSL as the only injury, one with only SSL injury, one with only unilateral OSL injury and one with SSL and OSL in combination.

Twenty-eight horses had concurrent injuries to other structures including:

Suspensory ligament branch injury (11), osteoarthritis of the fetlock (9/10 associated with P1 fracture or subchondral bone injury), subchondral bone injury of the fetlock (8), P1 fissure/fracture (7), DDFT tendinitis (6), navicular bone abnormalities (abnormal cystic shape and/or increased number (>7) of the synovial invaginations (2), fragment at the distal border (1), new bone formation at the proximal margin (1) and sagittal fracture (1)) (4), bursitis (4), distal interphalangeal joint synovitis (4), digital flexor tendon sheath tenosynovitis (4), distal metacarpus III fissure (1) and palmar annular ligament desmitis (1).

The CT and CE-CT image quality was considered adequate in all cases. Uptake of contrast medium was present in all major vessels.

Description of CT findings in the control horses

Precontrast CT

The shape of the SSL varied from proximal to distal, with the most proximal part having a triangular/crescent shape that rapidly became more oval in the proximal and mid aspect and rounded shape distally (Figures 1 and 2A).

The proximal part of the ligament had a homogeneous appearance with well-defined margins. In the mid-region, all ligaments had a moderate to markedly heterogeneous appearance containing multiple, focal, hypodense areas and with more ill-defined margins (Figure 2A).

Distally, the ligament regained a homogeneous (6/10) to mild heterogeneous (4/10) appearance with well-defined margins, and was joined by a soft tissue band medially and laterally (axial palmar ligament of the pastern joint) before merging with the middle scutum.

The medial and lateral OSL were triangular in shape at the most proximal aspect (Figure 1).

In their mid and distal parts, the ligaments had a crescent shape, with a convex palmar aspect and were located adjacent to the palmar/plantar bony surface of



Figure 1. Normal precontrast transverse CT image through the distal metacarpus III and the proximal aspect of the first phalanx, just distal to the proximal sesamoid bones. Medial is to the left. The proximal part of the SSL (*) has a well-defined triangular shape. The proximal part of the OSL (arrows) are triangular in shape and displays a heterogeneous appearance that is most pronounced at the axial aspect.

the proximal phalanx with a decreasing size towards their distal insertion (Figures 2A and 5A).

Proximally, the margins were poorly outlined, most pronounced at the dorsal aspect where the border merged with the soft tissue opacity of the cruciate and short sesamoidean ligaments. The axial aspect of the ligaments had a more hypodense appearance than the abaxial part and in some horses with focal hypodense areas.

At their mid and distal parts, the ligaments had a mild heterogeneous soft tissue attenuation. However, in 2/10 horses, focal hypodense areas were still present at the axial aspect of the lateral oblique sesamoidean ligament within the mid part. At the most distal aspect, the two ligaments merged together and continued as a single homogeneous structure until their insertion.

The axial branch of the OSL could not be separated from the SSL proximally, and was seen more distally as a small oval, ill-defined structure between the lateral and medial OSL. At the distal aspect, all three parts merged and inserted together at the palmar aspect of the proximal phalanx.

CE-CT findings

A fine network of small caliber, intra-ligamentous vessels were present within the proximal aspect of all OSL, immediately distal to their origin at the base of the proximal sesamoid bones (Figure 3A). More prominent vessels were located adjacent to the axial margin of the ligaments, extending to the dorsal aspect of the SSL, with vessels branching off towards the palmar margin of the proximal $\frac{1}{4}$ of the first phalanx. No contrast medium was detected within the mid and distal parts of the OSL (Figure 2B).

In 9/10 horses, a mild to moderate focal area of contrast enhancing vessels was present in the central aspect of the SSL, immediately distal to the proximal sesamoid bones (Figures 3A and 4A). This region appeared to be in continuation with a focal contrast enhancement within the palmar (intersesamoidean) ligament. Distally, the focal vessels extended towards the abaxial margins of the ligament to merge with the vessels at the axial margin of the OSL.

At the mid and distal parts, no obvious contrast en-

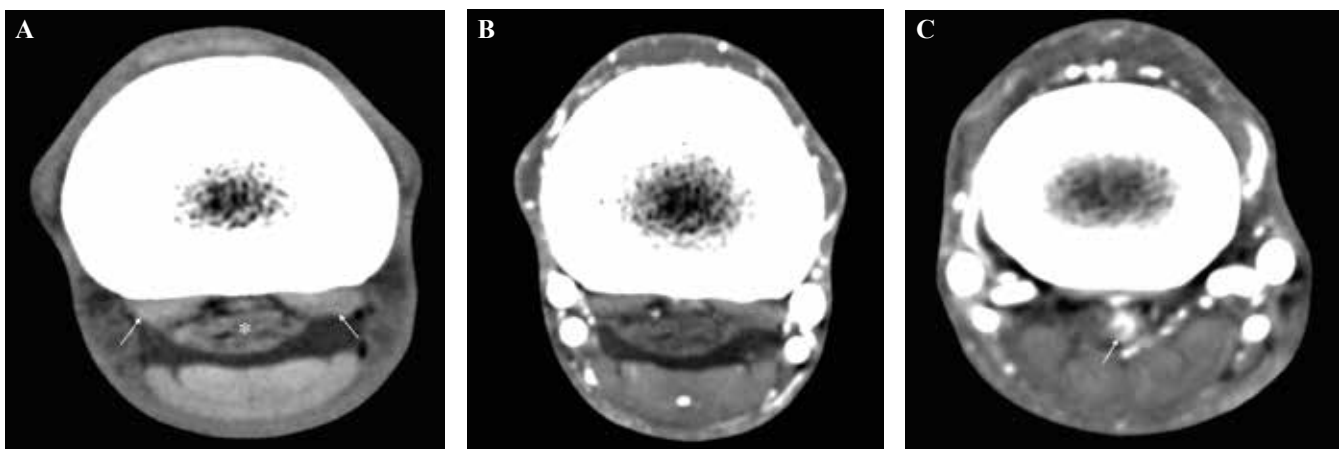


Figure 2. Computed tomography images through the proximal aspect of the first phalanx, displaying the mid part of the SSL. Medial is to the left on all images. A. Precontrast image of an unaffected SSL. The SSL (*) has an oval shape and a markedly heterogeneous appearance. This area should not be mistaken for an abnormal finding. The OSL (arrows) are triangular/crescent-shaped and are located adjacent to the bony surface of the first phalanx. B. Postcontrast transverse image of the same horse and level as in A. Medial is to the left. No contrast enhancement is seen within the SSL or OSL at this level. C. Abnormal postcontrast image. Moderate to marked, focal contrast enhancement is seen in the central and lateral aspect of the mid part of the SSL (arrow).

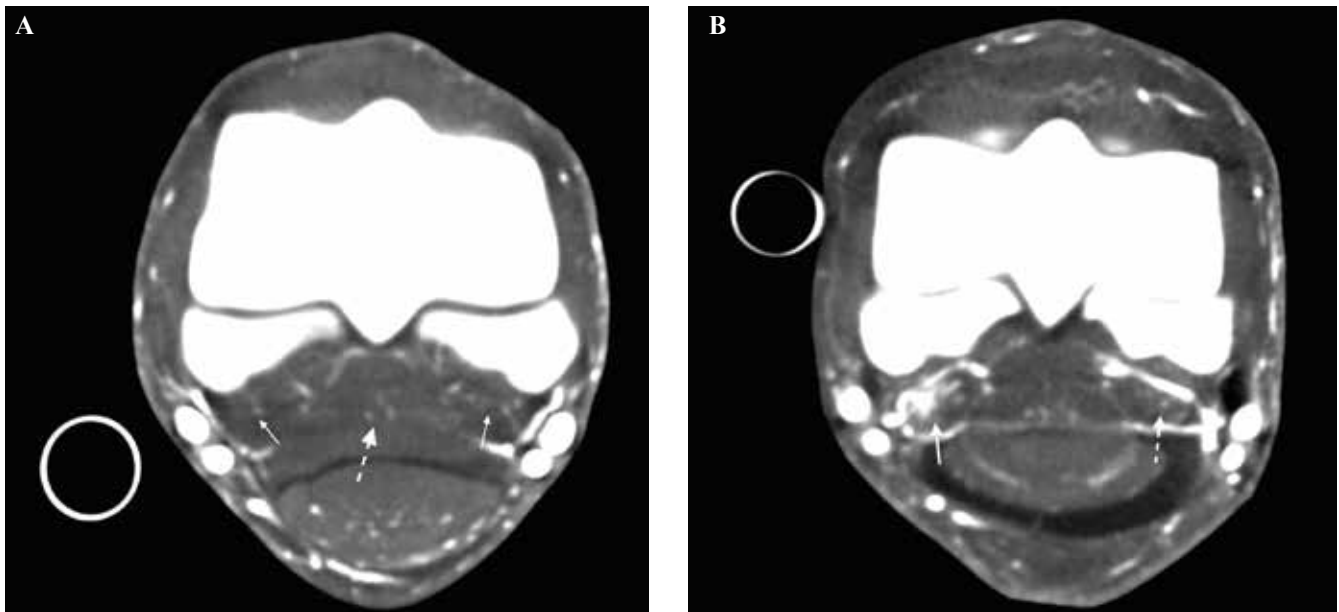


Figure 3. Computed tomography images through the distal metacarpus III and the proximal aspect of the first phalanx, just distal to the proximal sesamoid bones. Medial is to the left on all images. **A.** Postcontrast image of unaffected OSL. A network of small caliber, contrast-enhancing vessels are seen within the most proximal aspect of the OSL (solid arrows) as well as the central aspect of the SSL (interrupted arrow). **B.** Abnormal postcontrast transverse image at the same level as in A. There are marked contrast-enhancements of the MOSL (solid arrow), and to a lesser degree the LOSL (interrupted arrow).

hancements were detected within the SSL (Figure 2B). In 2/10 horses, a faint mid-sagittal vessel was seen extending through the ligament at approximately the mid aspect of the proximal phalanx.

At the middle half of the proximal phalanx, prominent contrast enhancing vessels were present at the dorsal and palmar aspect of the SSL, consistent with the palmar rami of the proximal phalanx. In one horse, an additional circumferential vessel was present immediately proximal to the palmar rami.

The bony surfaces at the level of the origin and insertion of unaffected ligaments was smooth.

Description of computed tomography findings of DSL injury

Precontrast CT findings of oblique sesamoidean ligaments

The affected ligaments appeared primarily heterogeneous in all regions: proximal (n=27/28), middle (n=27/28) and distal (n=21/28).

The margins were primarily poor to ill-defined in the proximal (21/28) and in the distal/middle region (18/28). The cross-sectional area subjectively appeared increased in all affected ligaments.

The appearance of the lesions on the precontrast CT examinations was either hypodense (16/28), hyperdense (7/28) or not detected (8/28).

Precontrast CT findings of the straight sesamoidean ligament

Eleven horses had abnormalities involving the proximal part, four the middle part and five the distal part of the SSL. Injury to the proximal part alone was seen in 7/13 cases and to the distal part alone in 2/13 cases. No horse had injury to the middle region alone. Four horses had injury involving a combination of the three regions.

The CT appearance of the affected ligament was either heterogeneous (9/13) or homogeneous (4/13) proximally, primarily heterogeneous (12/13) in the middle region and heterogeneous (9/13) distally.

The margins were well-defined proximally, and either ill-defined (6/13) or well-defined (7/13) in the middle and distal region. An increase in the cross-sectional area of injured ligaments was subjectively less obvious than for the OSL.

Subjective appearance of contrast-enhancing lesions on the precontrast CT examinations was either hypodense (11/13), hyperdense (1/13) or not detected (1/13).

Abnormalities associated with the bony insertions of the DSL were seen only in three horses. One horse had smooth new bone formation at the distal aspect of the insertion of the OSL. The other two horses had extensive periosteal proliferation at the palmar aspect of the proximal phalanx along the length of the OSL attachments.

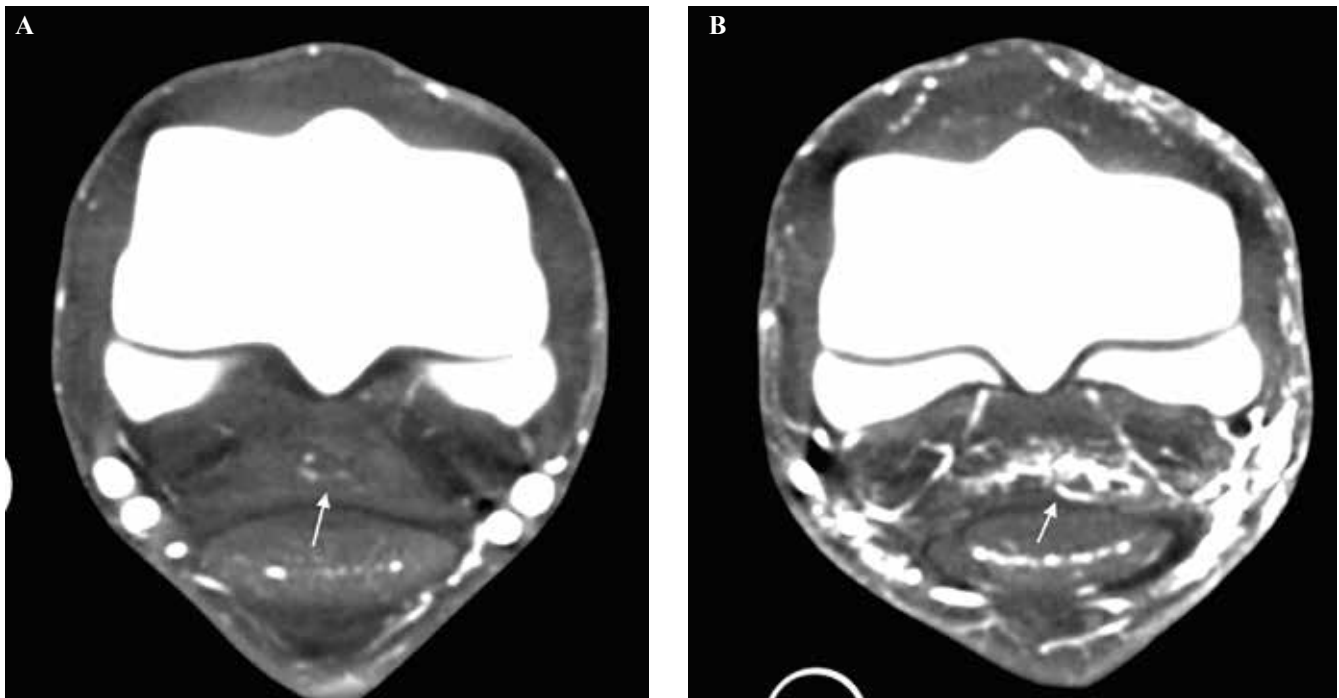


Figure 4. Computed tomography images through the distal metacarpus III and the proximal aspect of the first phalanx, just distal to the proximal sesamoid bones. Medial is to the left on all images. **A.** Postcontrast image of an apparently unaffected SSL. Mild contrast enhancement is seen in the central aspect of the proximal part of the SSL (arrow). **B.** Abnormal post contrast image. Marked, diffuse contrast enhancement is seen the entire aspect of the proximal part of the SSL (arrow).

Irregular proliferation and osseous resorption were also detected at the basilar region of the proximal sesamoid bones.

In one of the two horses, a clearly demarcated, lucent lesion with a central bone opacity (sequestrum) and marked surrounding irregular new bone formation was present at the mid aspect of the attachment of the LOSL.

CE-CT findings of the oblique sesamoidean ligaments

Contrast enhancement was subjectively graded as either mild (13/28) (Figure 5B), moderate (9/28) (Figure 5C) or severe (6/28) (Figure 3B).

The pattern of contrast enhancement was either focal (9/28) (Figure 5C) or diffuse (24/28), of which five were in combination. Contrast enhancement involved either the periphery (19/28) or central (21/28) region, with twelve being a combination of the two. Neovascularization was seen in 21/28 cases.

CE-CT findings of the straight sesamoidean ligament

Contrast enhancement was subjectively graded as either mild (3/13), moderate in (3/13) or severe (7/13) (Figure 4B).

The pattern of contrast enhancement was either focal (7/13) (Figure 2C), diffuse (8/13) (Figure 4B), of which two were in combination. Contrast enhancement involved either the periphery (8/13) or central

(12/13) region with 7 being a combination of the two. Neovascularization was seen in 10/13 cases.

DISCUSSION

In accordance with previous reports, injury to the OSL was more common than injury to the SSL in this study (Sampson et al., 2007; Gonzales et al., 2010; King et al., 2013). Thirty-two percent of the horses in this study had a combination of SSL and OSL injuries.

Contrary to previous reports, the incidence of both OSL and SSL injuries in this study were found to be higher in the front limbs (26/31, 84%), and were evenly distributed between right and left front limb. Schneider (2003) and King (2013) reported an even distribution between the front and hind limbs for SSL lesions, and the incidence of OSL lesions was found to be higher (67%) in the hind limbs (Sampson et al., 2017; King et al., 2013).

The distribution of lateral and medial OSL injury was overall similar for both unilateral and bilateral OSL injury in this study. However, for unilateral injury, the incidence of LOSL injury was 50% higher than of MOSL injury (lateral 8/28 and medial 4/28). This finding is contrary to the distribution found by Sampson (2007), where the medial OSL was found to be affected more often than the lateral in the front limbs.

Similar to previous reports, injury to the OSL was

more often seen in the proximal and mid part of the ligaments, and involvement of all three regions was seen in 21/28 horses. However, injury of the SSL was also seen more commonly in the proximal part in this study, which is in disagreement with a previous report (Sampson et al., 2007; Smith et al., 2008a).

Only three horses (10%) had DSL injury as the only injury. This finding is supported by the study of Smith (2008a), that similarly found DSL injury to be the sole cause of lameness in only 2/22 (9%) horses. In contrast, King (2012) reported a higher incidence of injury to the OSL alone, with solitary OSL injury in 56/232 horses (24%) and to the SSL in 38/232 horses (16%). Sampson (2007) found no other lesions in all included cases of DSL injury (n=27). However, it is unclear if the cases were included based on a solitary injury to the DSL.

The present study may not represent the overall prevalence of injury to this region, as it is possible that horses with more obvious abnormalities were diagnosed ultrasonographically and were hence not referred for CE-CT imaging.

The majority of horses in this study had concurrent injuries to other regions together with DSL injury. The most frequent injury combinations were suspensory ligament desmitis, subchondral injury of the metacarpophalangeal joint or P1 fissure with/without associated osteoarthritis of the joint. This finding is supported by other reports; however, the affected regions were not specified (Gonzales et al., 2010; King et al., 2013). In another study of concurrent injuries in horses with suspensory desmitis, 7/71 horses (7%) had concurrent injury to the OSL (Marneris et al., 2014).

These findings are most likely associated with the

biomechanical function of the metacarpophalangeal joint and the suspensory apparatus. The DSL are the functional continuation of the suspensory ligament, and it stands to reason that overload to this area would involve the DSL. The suspensory ligament prevents excessive extension of the metacarpophalangeal joint, and a close anatomical and biomechanical relationship exists between these structures (Denoix et al., 1994). Concurrent injury to the suspensory apparatus, including the DSL, and subchondral injury or incomplete fracture of the proximal phalanx are therefore not surprising.

Consequently, concurrent injuries to the DSL should be considered in horses presenting with fetlock trauma or suspensory branch injury.

The shape and the cross-sectional pattern (from proximal to distal) of both the SSL and OSL of the control group were similar to previous reports of both CT and MRI (Smith et al., 2008a; Vanderperren et al., 2008). The axial aspect of the OSL was often hypoattenuating and heterogeneous in comparison to the abaxial aspect, and care should be taken not to misinterpret it as a lesion.

The heterogeneous appearance of the mid aspect of the SSL is marked in comparison to the proximal and distal regions. Fibers of the DSL are not as compact as the tendon fibers. The heterogeneous appearance is considered the result of the adipose and loose connective tissue present between the ligament fibers (Kleiter et al., 1999). Additionally, a fibrocartilage component has been found histologically within the origin of the DSL, similarly to the insertional region of the suspensory ligament and the deep digital flexor tendon (DDFT) (Kleiter et al., 1999).

The fibrocartilaginous part of the distal DDFT has

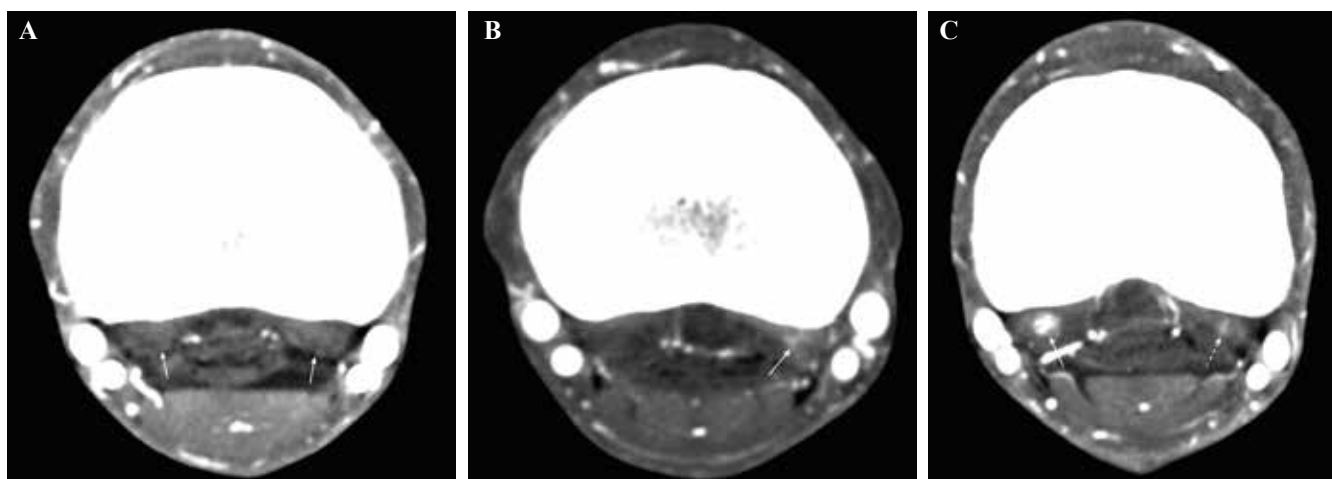


Figure 5. Computed tomography images through the proximal aspect of the first phalanx. Medial is to the left on all images. **A.** Postcontrast image of unaffected OSL. The OSL are triangular/crescent shaped and located adjacent to the bony surface of the first phalanx (arrows). No contrast enhancement is detected within the ligaments. **B.** Abnormal postcontrast image of the OSL. A mild, diffuse contrast enhancement is seen within the abaxial aspect of the LOSL (arrow). **C.** Abnormal postcontrast image of the OSL. A moderate, focal area of contrast enhancement is in the central aspect of the MOSL (solid arrow). A mild, diffuse contrast enhancement is also seen within the LOSL (interrupted arrow).

been found to be less attenuating than the fibrous part, which may explain the proximal appearance in the present study (Claerhoudt et al., 2014).

CT imaging is performed with the horse anesthetized and in lateral recumbency. Therefore, the orientation of the limb does not reflect the natural standing orientation of the limb. In a non-weight bearing horse, the ligaments and tendons are not under tension, and the resulting relaxation during non-weight bearing may potentially influence the size, shape and attenuation pattern.

The axial branch of the OSL has previously been described, and is thought to be a component of the OSL (Denoix, 2000). In the present study, this ligament could not be separated from the SSL proximally, and appeared to arise from the SSL. Distally, the ligament was located axially to the OSL and inserted together with the OSL distally.

In control horses, small caliber, intra-ligamentous vessels were present within the most proximal aspect of the OSL. No contrast material was detected within the OSL at any other location in these ligaments in control horses, and caution is advised in considering these interligamentous vessels an abnormal finding. Further studies of clinically normal horses are needed to determine if this finding is related to the normal vascular anatomy of this region. A very focal contrast enhancing area was detected within the central part of the SSL just distal to the proximal sesamoid bones in almost all control horses, often extending to the intersesamoidean ligament. Given the consistency of this appearance, it most likely represents normal vascular anatomy. No obvious contrast enhancement was seen in the mid and distal parts of the SSL in horses with only injury to the OSL.

In all affected ligaments, the contrast enhancement was clearly detected within the ligaments in regions that did not show contrast enhancement in control horses. Within the proximal part of injured DSL, focal or diffuse areas of contrast were detected within the ligament, and/or the degree of intra-ligamentous vessels seen in control horses were subjectively increased and contrast enhancements extended distal to this region. A varying degree of neovascularization was seen in most cases.

The majority of the lesions observed on postcontrast examination were not or barely visible on the precontrast images, but were usually seen as slightly hypoattenuating areas.

Damage and inflammation of tendinous or ligamentous structures are anticipated to cause contrast enhancement, leading to an increased conspicuity of abnormalities within these structures.

Intravascular contrast enhancement is thought to be due to a change in tissue permeability and neovascularization, both known to be important aspects of tendon and ligament injury and repair (Pollard et al., 2004; Sharma and Maffulli 2005; Dawson et al., 2006).

In one horse, a contrast-enhancing lesion in the DDFT has previously been found to represent densely packed small caliber endothelial vessels residing in granulation tissue either replacing or separating the normal fiber bundles (Puchalski et al., 2009).

Limitations of this study exist and are primarily due to the retrospective study design and the lack of a non-lame control group. A complete history of lameness duration and response to local anesthesia were not always available for the included horses. Additionally, many of the included horses were referral cases and the clinical examinations and additional diagnostic imaging were not performed at the hospital and thus unavailable for review. For this reason, little or no emphasis was placed on the lameness score or duration, as well as radiographic and ultrasonographic examinations. The purpose of this study was not to describe the CE-CT findings of DSL as a solitary injury causing lameness, but to describe the abnormal findings of these ligaments compared to a group of horses without injury to the DSL. Additionally, ultrasonography has been shown to be less sensitive for detection of DSL injury (Schneider et al., 2003; Sampson et al., 2007; Smith et al., 2008a). In the study of Smith (2008a), MRI abnormalities of the DSL were not detected using ultrasound in 80% of the cases. Radiography is useful to detect abnormalities of the ligamentous insertion; however, CT is inherently more sensitive given the 3D nature of the modality.

According to other studies, the response to regional anesthesia of the distal limb in horses with DSL injury are variable, ranging from a positive response to distal digital nerve block to a low palmar (low 4-point) (Schneider et al., 2003; Sampson et al., 2007). This could reflect a difference in injury location (proximal or distal), or the range of diffusion of the local anesthetic product. However, with exception for anesthesia of the digital flexor tendon sheath (DFTS), the response to regional anesthesia does not seem to be consistent for these injuries (Sampson et al., 2007). Additionally, given the complex of injuries detected in this study, the response to local anesthesia would be expected to be inconsistent.

Clinical presentation, treatments and prognosis of injuries to the DSL have been covered elsewhere (Schneider et al., 2003; Sampson et al., 2007).

Because of the variation between individual horses, both limbs should ideally have been imaged. However, given the retrospective nature of this study, this was not available.

Horses without history of lameness were not examined, as the control horses were lame. However, all control horses had significant injury to the foot region or responded to anesthesia of the distal interphalangeal joint or the navicular bursa. It was therefore considered that the DSL were normal, although a subclinical injury of this region cannot be excluded.

Several horse breeds were included in this study,

including ponies. It is possible that the smaller height and body weight may have increased the variations of the cross-sectional area. In this study, a correlation between weight, height and measurement was not addressed. The cross-sectional area of the SSL has been found to be positively associated with both height and weight, but the cross-sectional area of the OSL was only statistically associated with height at the proximal part (Smith et al., 2008a).

Ideally, pathology or histopathology confirmation of the lesions should have been performed; however, this was not possible, making the diagnosis of DSL injury deductive.

At this time, there are a limited number of reports describing the use of CE-CT for evaluation of normal or abnormal findings of the distal extremity of the horse.

MRI is generally considered the gold standard of soft tissue orthopedic imaging. However, some limitations of the modality exist, such as inherent long scanning times and magic angle artifact, which have been shown to affect the OSL in standing MRI (Smith et al., 2008b). Moreover, in many equine hospitals, only one cross-sectional imaging modality may be available due to economical considerations.

In a study comparing CE-CT and low field MRI of horses with foot lameness, contrast enhancement was commonly identified in soft tissue structures of lame horses. Lesion detection varied depending on the lesion location; however, lesions of the DDFT were identified more often with CT/CECT than the low field MRI (Vallance et al., 2012).

In the present study, the authors found that there was a clear difference in the contrast enhancement of the DSL between case horses and controls. The heterogeneous appearance of some regions may potentially be misinterpreted as a lesion, and CE-CT can be helpful in differentiating between abnormalities and normal anatomy.

CE-CT has the potential to increase the diagnostic utility of CT for soft tissue lesions; however, contrast enhancement in desmopathy is still a novel technique and further studies are needed to better understand the significance of these findings.

REFERENCES

Bergman E.H.J., Puchalski S.M., van der Veen H., Wiemer P. (2007). Computed tomography and computed tomography arthrography of the equine stifle: technique and preliminary results in 16 clinical cases. In: *AAEP Proceedings* 53, 46-55

Claerhoudt S., Bergman E.H.J., Saunders J.H. (2014). Computed tomographic anatomy of the equine foot. *Anatomia, Histologia, Embryologia* 43, 395-402

Collins J.N., Galuppo L.D., Thomas H.L., Wisner E.R., Hornof, W.J. (2004). Use of computed tomography angiography to evaluate the vascular anatomy of the distal

portion of the forelimb of horses. *American Journal of Veterinary Research* 65, 1409-1420

Dawson P. (2006). Functional imaging in CT. *European Journal of Radiology* 60, 331-340

Denoix J.M., Crevier N., Azevedo C. (1991). Ultrasound examination of the pastern. In: *AAEP Proceedings* 37, 363-379

Denoix, J.M. (1994). Functional anatomy of the tendons and ligaments in the distal limbs. *Veterinary Clinics of North America: Equine Practice* 10, 273-322

Denoix J.M. (2000). The equine pastern. In: Denoix JM (editor). *The Equine Distal Limb: an Atlas of Clinical Anatomy and Comparative Imaging*. Manson Publishing Ltd., London, p 129-241.

Dyson S.J., Denoix J.M. (1995). Tendon, tendon sheath, and ligament injuries in the pastern. *Veterinary Clinics of North America: Equine Practice* 11, 217-233.

Gonzalez L.M., Schramme M.C, Robertson I.D., Thrall D.E., Redding R.W. (2010). MRI features of metacarpo(tarso)phalangeal region lameness in 40 horses. *Veterinary Radiology & Ultrasound* 51, 404-414

King J.N., Zubrod C.J., Schneider R.K., Sampson S.N, Roberts G. (2013). MRI findings in 232 horses with lameness located to the metacarpo(tarso)phalangeal region and without a radiographic diagnosis. *Veterinary Radiology & Ultrasound* 54, 36-47

Kleiter M., Kneissl S., Stanek C., Mayrhofer E., Baulain U., Deegen E. (1999). Evaluation of magnetic resonance imaging techniques in the equine digit. *Veterinary Radiology & Ultrasound* 40, 15-22

Marneris D., Dyson S.J. (2014). Clinical features, diagnostic imaging findings and concurrent injuries in 71 sports horses with suspensory branch injuries. *Equine Veterinary Education* 26, 312-321

Pollard R.E., Gracia T.C., Stieger S.M., Ferrara K.W., Sadowski A.R., Wisner E.R. (2004). Quantitative evaluation of perfusion and permeability of peripheral tumors using contrast-enhanced computed tomography. *Investigative Radiology* 39, 340-349

Puchalski, S.M., Galuppo, L.D., Hornof, W.J. and Wisner, E.R. (2007). Intraarterial contrast-enhanced computed tomography of the equine distal extremity. *Veterinary Radiology & Ultrasound* 48, 21-29

Puchalski S.M., Galuppo L.D., Drew C.P., Wisner E.R. (2009). Use of contrast-enhanced computed tomography to assess angiogenesis in deep digital flexor tendonopathy in a horse. *Veterinary Radiology & Ultrasound* 50, 292-297

Sampson S., Schneider R., Tucker R., Gavin P., Zubrod C., Ho C. (2007). Magnetic resonance imaging features of oblique and straight distal sesamoidean desmitis in 27 horses. *Veterinary Radiology & Ultrasound* 48, 303-311

Schneider R., Tucker R., Habegger S., Brown J., Leathers C. (2003). Desmitis of the straight sesamoidean ligament in horses: 9 cases (1995-1997). *Journal of the American Veterinary Medical Association* 222, 973-977

Sharma P., Maffulli N. (2005). Tendon injury and tendinopathy: healing and repair. *The Journal of Bone and Joint Surgery* 87, 187-202

Smith S., Dyson S.J., Murray R.C. (2008a). Magnetic resonance imaging of distal sesamoidean ligament injury. *Veterinary Radiology & Ultrasound* 49, 516-528

Smith S., Dyson S.J., Murray R.C. (2008b). Is magic angle effect observed in the collateral ligaments of the distal in-

terphalangeal joint or the oblique sesamoidean ligaments during standing magnetic resonance imaging? *Veterinary Radiology & Ultrasound* 49, 509-515

Pollard R., Puchalski S. (2011). CT contrast media and applications. In: Schwarz, T. and Saunders J. (editors). *Veterinary Computed Tomography*. John Wiley & Sons Ltd., West Sussex, p 57-65.

Vallance S.A., Bell R.J.W., Spriet M., Kass P.H., Puchalski S.M. (2011). Comparisons of computed tomography, contrast-enhanced computed tomography and standing

low-field magnetic resonance imaging in horses with lameness localized to the foot. *Equine Veterinary Journal* 44, 149-156

Vanderperren K., Ghaye B., Snaps F.R., Saunders J.H. (2008). Evaluation of computed tomographic anatomy of the equine metacarpophalangeal joint. *American Journal of Veterinary Research* 69, 631-638

Vind de juiste werker voor je bedrijf

www.mediaservice.be

Plaats je
personeelsadvertentie in
Vlaams Diergeneeskundig Tijdschrift
en krijg 15% korting.



129418M00033 © SHUTTERSTOCK

Mediaservice 
gericht adverteren